SUBSALT IMAGING WITH ACOUSTIC AND ELASTIC 2D FULL WAVEFORM INVERSION

N. Thiel, A. Przebindowska, A. Kurzmann, and T. Bohlen

email: *niklas.thiel@kit.edu*

keywords: *subsalt imaging, full waveform inversion, flooding technique, acoustic, elastic*

ABSTRACT

The aim of this study is to apply the Full Waveform Inversion (FWI) to the problem of subsalt imaging. We perform a synthetic test with acoustic and elastic FWI in presence of acoustic and elastic data. The choice of a starting model and the influence on the FWI results are studied. We also further develop and apply the Flooding Technique for the subsalt imaging problem.

In this study we identify potential problems of the starting model for the FWI and show how accurate information about shape and location of the salt body are required in the starting model. We show that the acoustic FWI with acoustic data and the elastic FWI with elastic data is able to image the subsalt area sufficiently, if the salt body is included in the starting model. The accordance of the FWI results and the true model is very high. The acoustic inversion of elastic data is not successful and produces many artefacts.

By using the Flooding Technique within the framework of acoustic FWI with acoustic data, very good imaging results for the subsalt part can be achieved. This technique does not require information about the salt body in the starting model. For the acoustic FWI with elastic data the Flooding Technique is not successful in imaging the subsalt area.

INTRODUCTION

The demand for hydrocarbons is huge and will continue to be huge in the next years. Therefore, energy companies keep looking for new reservoirs but the discovery of new hydrocarbons becomes increasingly challenging (Leveille et al., 2011). In the past, salt basins proved to be successful sites for the search. The most well-known site of salt basins in connection with hydrocarbons is the Gulf of Mexico (GoM).

For classical imaging techniques the reconstruction of structures beneath or near salt bodies is challenging (e.g., Ravaut et al., 2008). The main reason is the geomechanical characteristics of salt bodies. The salt was deposited millions of years ago and other sediments deposited on top. Using openings in the sediments on top of the salt layer the salt moved upwards, driven by the surcharge, and formed canopies. Therefore, the shapes of salt bodies and salt layers are normally very complex. In addition to the shape, the allochthonous salt layers often contain trapped sediments and have a rugose surface (Leveille et al., 2011). The intricate shapes and surfaces of salt bodies result in a complex wave propagation. Regions of poor illumination are often present. Additionally, the energy coming up from subsalt regions is weak due to high reflection coefficients at the sediment-salt interfaces. Therefore, classical imaging techniques have problems picturing the flanks, the bottom of the salt and the subsalt area. Consequences could be geological misinterpretations which are very expensive (Ravaut et al., 2008).

For some subsalt imaging problems solutions have already been developed, such as undershooting for smaller salt bodies by using longer offsets. For salt layers even this technique is not applicable. A promising solution for the problem of subsalt imaging is the application of Full Waveform Inversion (FWI). Unlike conventional techniques the entire waveform is used in the FWI approach. Synthetic data is modelled by using a starting model of the subsurface beneath the acquisition profile. The synthetic data is compared with the field data. In order to match the synthetic data to the field data the starting model is updated iteratively. The FWI can help, depending on the acquisition geometry and recorded waves, to improve the depth image considerably, in particular the subsalt area.

In this work the 2D acoustic (e.g., Tarantola, 1984) as well as the 2D elastic FWI in time domain (e.g., Tarantola, 1986; Mora, 1987) is used. The FWI is applied on synthetic marine data, based on a 2D seismic line from the GoM, delivered by Fugro (Fugro Multiclient Services, now part of CGG). The main focus is on the reconstruction of subsalt structures such as horizontal layers and steep dipping structures.

The most simple and fastest approach for the FWI is the usage of acoustic FWI in combination with synthetic acoustic field data. Different starting models and their influence on the FWI result are tested. This study answers questions about the required quality of a starting model for a successful FWI. The Flooding Technique is investigated in detail. This multi-stage inversion strategy requires no a priori information about the salt body. The original approach of Boonyasiriwat et al. (2010) is compared with the modified Flooding Technique proposed in this work.

As the assumption of acoustic field data is unrealistic the acoustic FWI is applied to elastic data. Especially for large data sets the acoustic FWI is not as expensive as the elastic FWI (Vigh et al., 2009). The FWI experiment uses a starting model including the salt at the exact location and with the correct shape. In order to compare the acoustic and elastic data the elastic data was converted in pressure data. The comparison revealed an increase of the data differences with offset. Therefore, a limitation of the offset is analysed. The results of the modified Flooding Technique using the acoustic FWI with elastic data are discussed.

PREPARATION

For the synthetic tests we use a salt body from a migration model delivered by Fugro. The salt body spreads over the full width of the model. The true background model is a subpart of the sigsbee2A model with a size of about 10 km in x direction and 6 km in depth. The used frequency content is in a range of 3-10 Hz.

The v_S and density models were calculated from the v_P model, shown in figure 1. The parameter models consist of an equidistantial grid with 850 grid points in x direction and 532 grid points in depth direction. The grid spacing is 12.5 m.

The acquisition geometry is based on the real acquisition geometry and has the feature of a long far offset of 9.5 km for the last shot. The acquisition geometry consists of 50 shots with an increasing number of receivers (16 to 751 receivers per shot).

ACOUSTIC INVERSION WITH ACOUSTIC DATA

In the starting model test the required correctness of the starting model for a successful inversion was studied. By using a 1D linear gradient as background model and the correct salt body in the correct location in the starting model, the true model can be reconstructed very well by the acoustic FWI with acoustic data (figure 2(c)). The area above the salt body is reconstructed almost perfectly and the subsalt area can be reconstructed. All sedimentary layers and steep dipping structures can be resolved. This example shows the high potential of the FWI pertaining the subsalt imaging problem.

If the starting model contains no information of the salt body the FWI fails (figure 2(d)). Only a rough top salt line can be reconstructed and the upper part of the model contains various artefacts. In the subsalt part no structures can be reconstructed. Apparently more information about the salt body are necessary to perform a successful FWI.

To estimate the required preciseness of these information the salt body was shifted up in the starting model (figure 3(f)). This study shows that even a shifting of the salt body smaller than one wave length (75 m) produces artefacts in the resulting model. The greater the shifting the higher are the amount of artefacts, especially in the upper part of the model, produced by the cycle skipping effect. The amount of artefacts can be reduced for small displacements (up to one wave length) of the salt body by introducing a transition zone at the sediment-salt boundary.

To avoid the requirement of precise information of the salt body the Flooding Technique (Boonyasiriwat et al., 2010) was applied. The Flooding Technique is a multistage inversion strategy reconstructing the model in three stages:

- first stage: FWI with a starting model without salt body

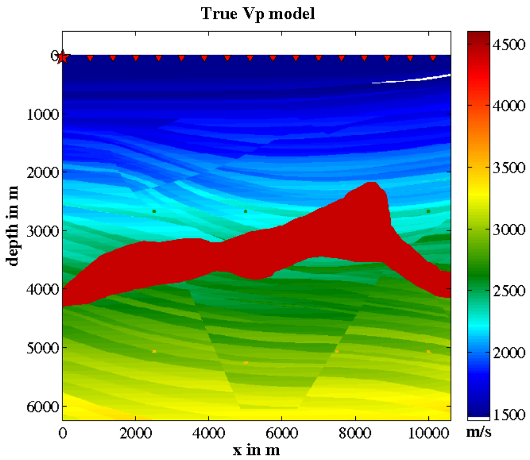

(a) True v_P model.

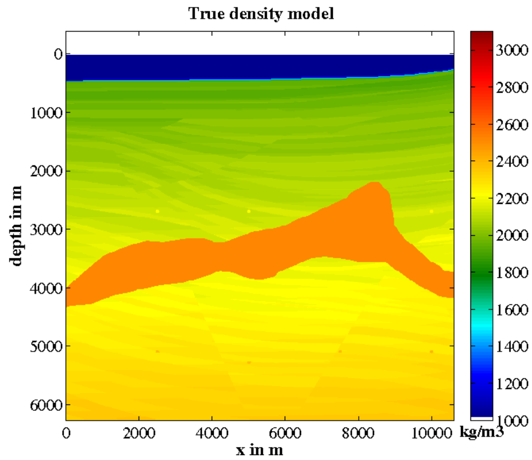

(b) True density model.

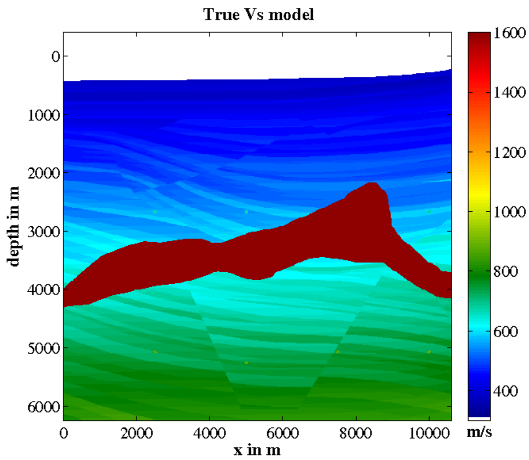

(c) True v_S model. The salt body velocity is 2600 $\frac{\text{m}}{\text{s}}$.

Figure 1: Modified part of the Sigsbee2A model including the salt body.

- second stage: picking the top line of the salt body in the result of the first stage and flood the area below with salt velocity before applying the FWI
- third stage: picking the bottom line of the salt body in the result of the second stage and flood the area below with sediment velocity before applying the FWI

In the result of the Flooding Technique the salt body can be reconstructed with a location error of 50-75 m (figure 4). The edges of the salt body have a greater error due to the linear extrapolation. The poor matching at the sides of the model does not influence the remaining part of the model notably, because the illumination, and therefore the information content of these parts in the data, is very small. A few artefacts are visible but considerably less than in the FWI with the mislocated salt body in the starting model. In the subsalt part the thicker layers can be reconstructed and also the steep dipping structures are slightly visible.

A lower location error of the salt body is one possibility to enhance the imaging result in the subsalt part. Therefore, the original Flooding Technique was modified:

- a 2D lowpass filter applied on the model and the correction of pronounced artefacts
- a smoothed sediment-salt transition zone
- flooding with a gradient in the subsalt area

- reconstruction from shallow to deeper parts (time windowing)

In the result of the modified Flooding Technique the upper part of the model contains almost no artefact (figure 5 and 6). The location error of the salt body is below 50 m, apart from the model sides including the extrapolations. The layers in the subsalt area are also better resolved than in the result of the original Flooding Technique. The FWI can adapt the velocities in the layers to the real velocity and not only relative velocity changes.

The modified Flooding Technique produces realistic FWI result by reconstruction the salt body without any a priori information about the salt body. The last stage of the modified Flooding Technique can reconstruct the layers and faults in the subsalt area very well.

ACOUSTIC INVERSION WITH ELASTIC DATA

A more realistic approach is the usage of elastic data. As the acoustic FWI is the fastest way with relative low computational cost, this method is used first. As supposed, the acoustic FWI with elastic data produces results containing many artefacts (figure 7(a)). The artefacts are the results of the attempt to explain the elastic data with acoustic data. By varying the parameters of the FWI the artefacts can be reduced but not prevented completely. In the subsalt area, only the thicker layers can be reconstructed. The steep dipping structures are not visible. The following parameters were modified:

- using normalised L2 norm instead of L2 norm
- apply additionally a 2D median filter to the starting model (filter size: 5 grid points)
- reduce maximum deviation from starting model (v_P and ρ) to 20%

The Flooding Technique produces also results with a great amount of artefacts (figure 7(b)). The salt body is not constructed as precisely as with acoustic data. Structures in the subsalt area can be reconstructed only partly.

ELASTIC INVERSION WITH ELASTIC DATA

The acoustic FWI of elastic data cannot reconstruct the subsalt area successfully. Therefore, the elastic FWI was applied on the elastic data. Firsts test have shown that the FWI results of the elastic FWI are comparable to the results obtained with the acoustic FWI of acoustic data (figure 8). The results are optically identical and the relative model error is very similar. Another advantage is the result of a v_S model. A successful FWI on v_P and v_S waves can deliver important information for fluid or gas reservoirs in the subsalt area. The first elastic FWI for only 40 iterations produces a v_S model with weak updates. First structures are visible in the upper part above the salt body. Further iterations will probably lead to a better v_S model result.

CONCLUSIONS

In this synthetic study we used 2D Full Waveform Inversion to investigate the problem of subsalt imaging. We applied successfully acoustic FWI to acoustic data as well as elastic FWI to elastic data. Here, the salt body is included in the starting model at the right location. The subsalt part can be imaged very precisely and the resulting model shows high accordance with the true model. The impact of a potential location error of the salt body in the starting model on the FWI results is considerably. Only for small location errors the artefacts in the results can be reduced by a smoothed sediment-salt transition zone. If the salt body is missing completely in the starting model, the FWI failed.

Therefore, the Flooding Technique was further developed and successfully applied in the acoustic FWI with acoustic data. In this multistage inversion strategy the knowledge of the salt body location is not necessary. The model recovery starts with shallow and continues with deep parts including the subsalt area. By using the Flooding Technique for the acoustic FWI with elastic data the result was not satisfactory. Many artefacts occur in the results and the subsalt part cannot be reconstructed.

ACKNOWLEDGMENTS

This work was kindly supported by the sponsors of the *Wave Inversion Technology (WIT) Consortium*. We also thank Fugro Imaging Ltd. (now part of CGG) for the provision of the data including all necessary information. The inversions were performed on the JUROPA cluster at Jülich supercomputing centre.

REFERENCES

Boonyasiriwat, C., Schuster, G. T., Macy, B., Valasek, P., and Cao, W. (2010). Application of multi-scale waveform inversion to marine data using a flooding technique and dynamic early-arrival windows. *Geophysics*, 75(6):R129–R136.

Leveille, J. P., Jones, I. F., Zhou, Z.-Z., Wang, B., and Liu, F. (2011). Subsalt imaging for exploration, production, and development: A review. *Geophysics*, 76(5):WB3–WB20.

Mora, P. (1987). Nonlinear two-dimensional elastic inversion of multioffset seismic data. *Geophysics*, 52(9):1211–1228.

Ravaut, C., Alerini, M., Pannetier-Lescoffit, S., and Thomassen, E. (2008). Sub-salt imaging by full-waveform inversion: a parameter analysis. In *2008 SEG Annual Meeting*.

Tarantola, A. (1984). Inversion of seismic reflection data in the acoustic approximation. *Geophysics*, 49(8):1259–1266.

Tarantola, A. (1986). A strategy for nonlinear elastic inversion of seismic reflection data. *Geophysics*, 51(10):1893–1903.

Vigh, D., Starr, E. W., and Elapavuluri, P. (2009). Acoustic waveform inversion vs. elastic data. In *2009 SEG Annual Meeting*.

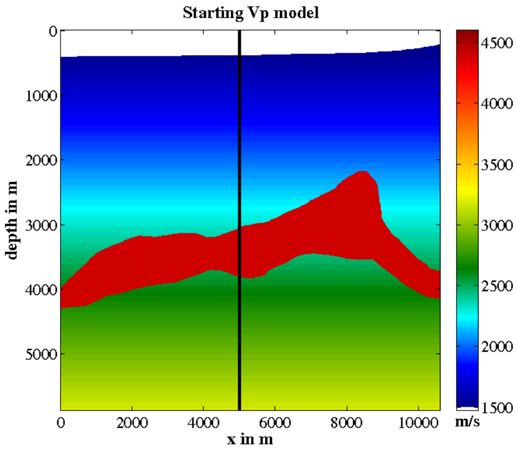

(a) v_P starting model including the salt body.

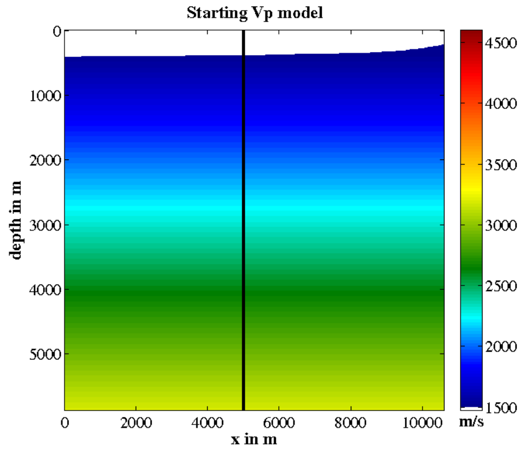

(b) v_P starting model with no salt body.

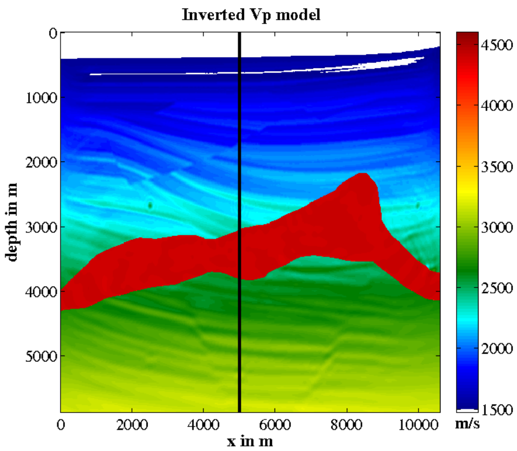

(c) v_P inversion result after 400 iterations (saltbody included in the starting model).

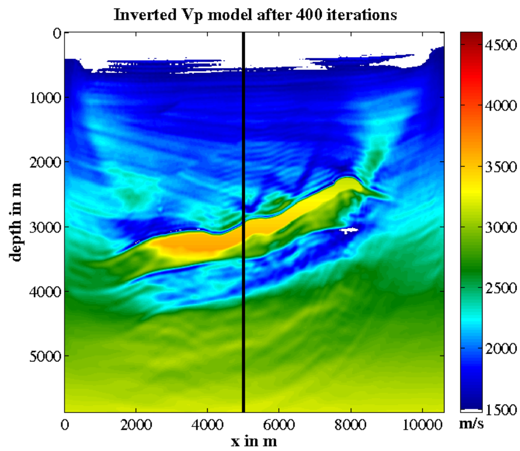

(d) v_P Inversion result after 400 iterations with no starting model.

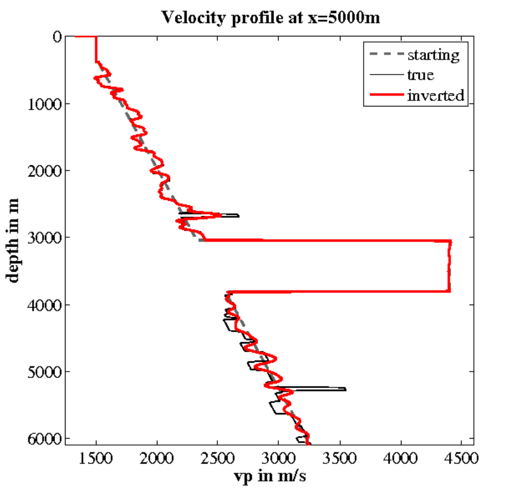

(e) Velocity profile located at the black line in Figure 2(c).

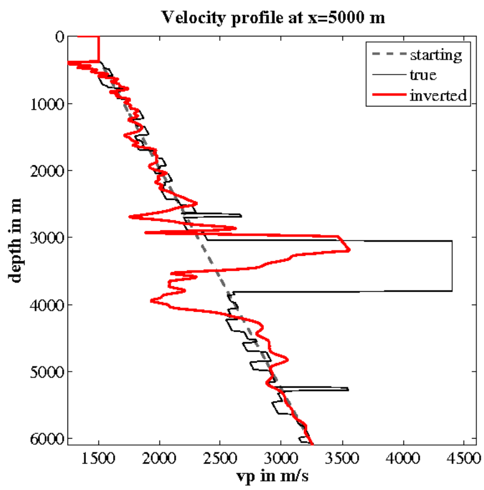

(f) Velocity profile located at the black line in Figure 2(d).

Figure 2: Test result with different starting model.

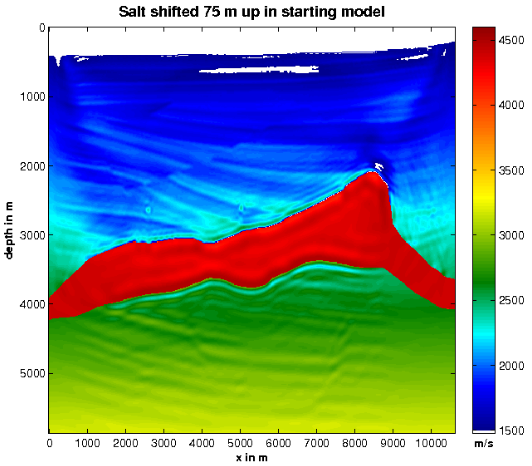

(a) Salt body shifted up by 75 m, hard sediment-salt transition.

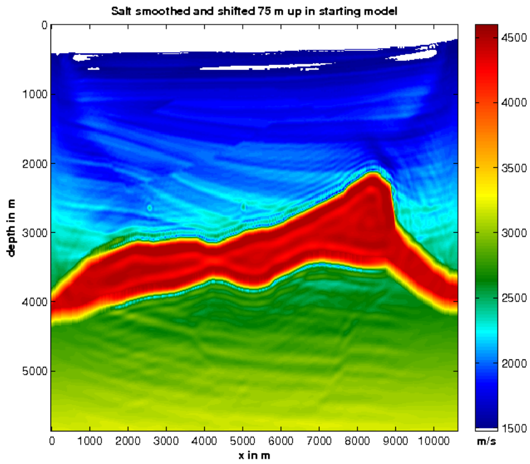

(b) Salt body shifted up by 75 m, smoothed sediment-salt transition.

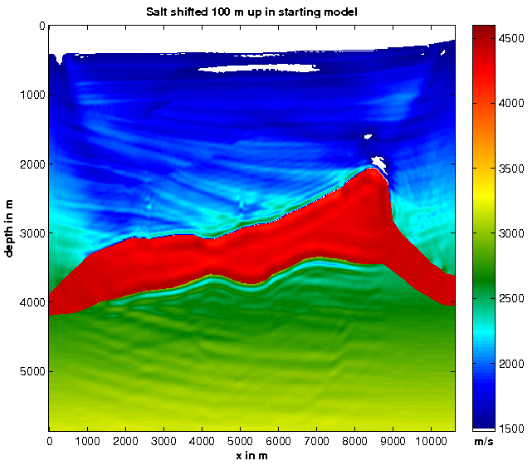

(c) Salt body shifted up by 100 m, hard sediment-salt transition.

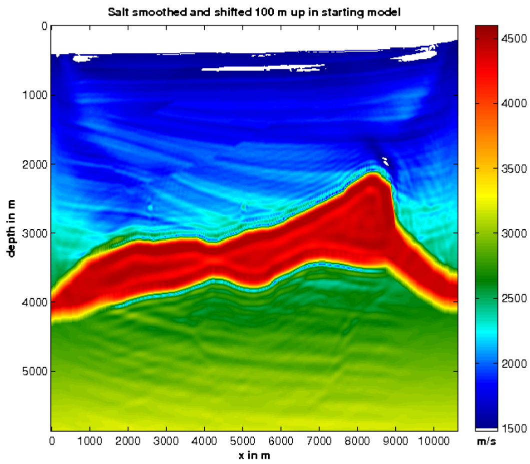

(d) Salt body shifted up by 100 m, smoothed sediment-salt transition.

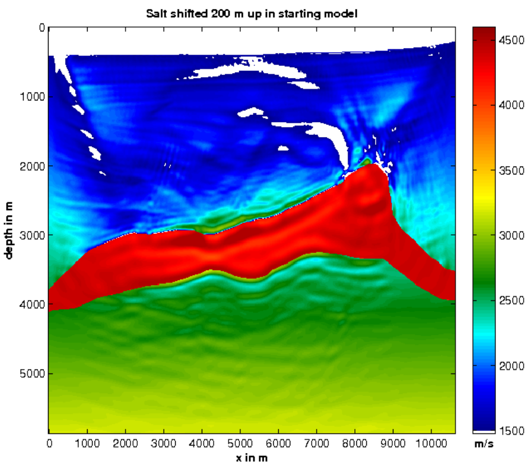

(e) Salt body shifted up by 200 m, hard sediment-salt transition.

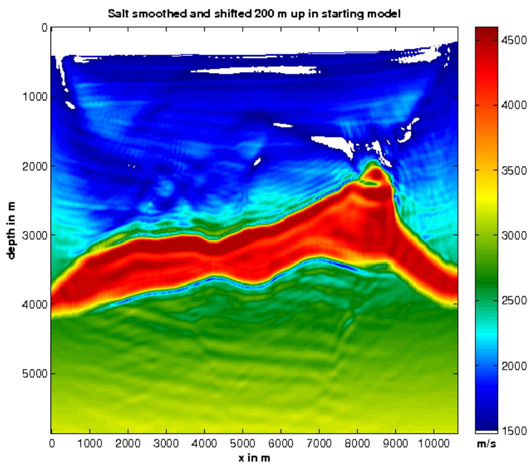

(f) Salt body shifted up by 200 m, smoothed sediment-salt transition.

Figure 3: Comparisons of FWI results for the v_P model with various shifts of the salt body in the starting models.

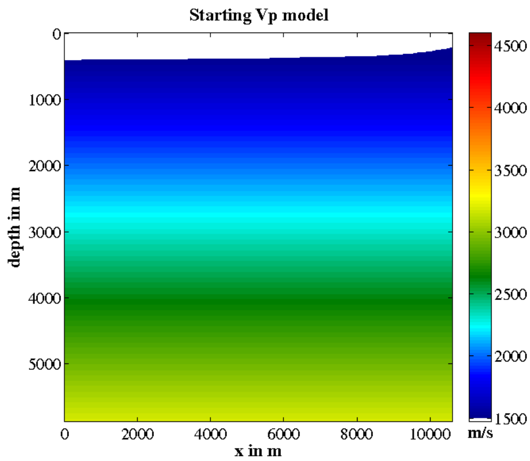

(a) Starting model for the first FWI stage.

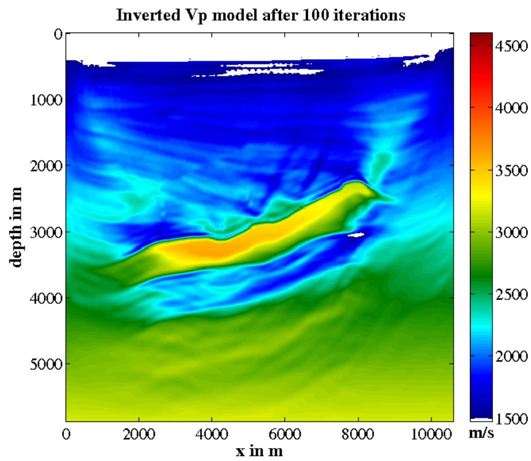

(b) Result after the first FWI stage.

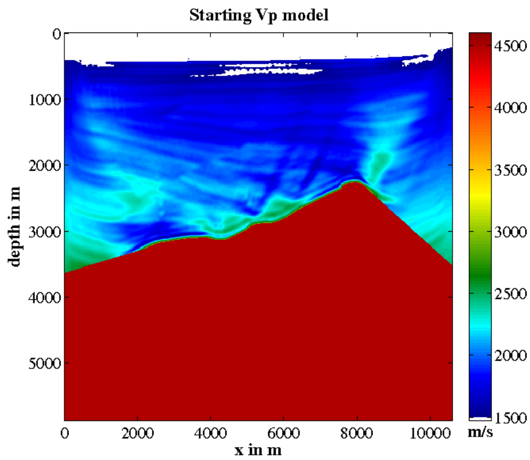

(c) Starting model for the second FWI stage.

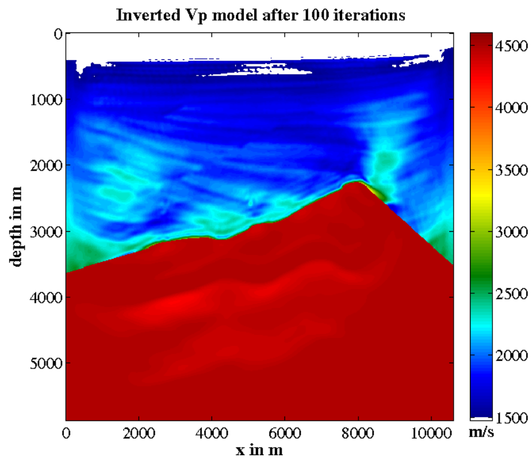

(d) Result after the second FWI stage.

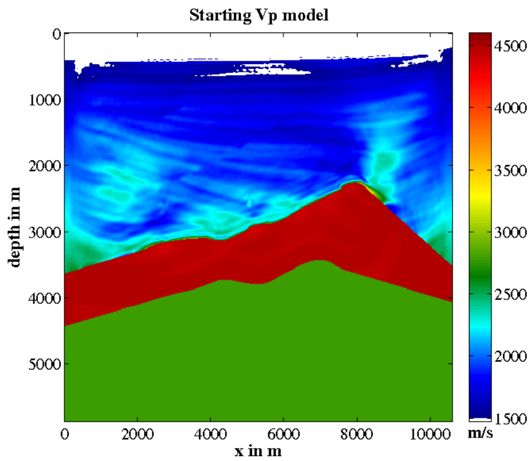

(e) Starting model for the third FWI stage.

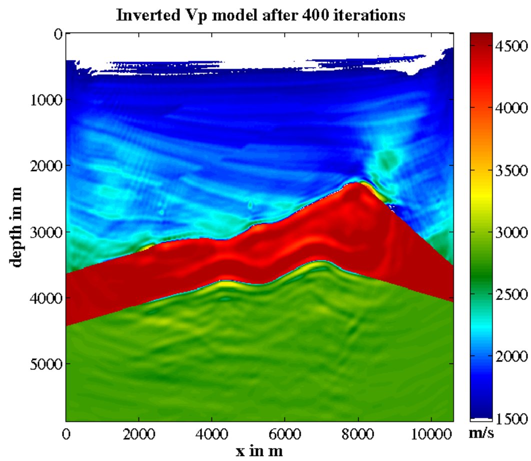

(f) Result after the third FWI stage.

Figure 4: P-wave velocity model at different stages of the original Flooding Technique after Boonyasiriwat et al. (2010).

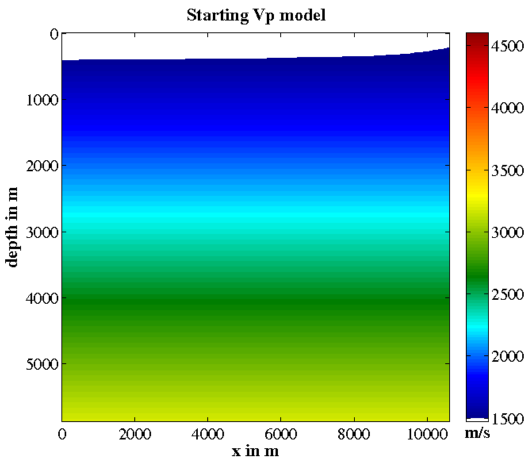

(a) Starting model for the first FWI stage.

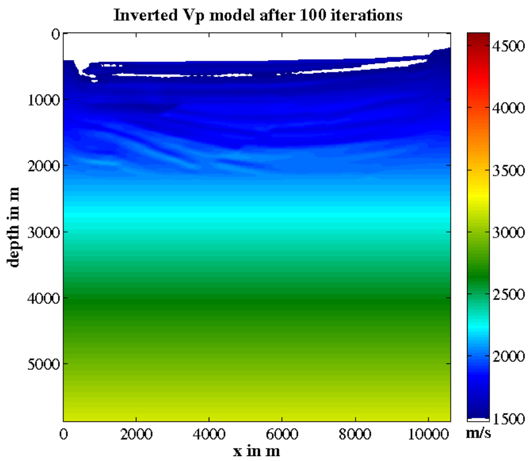

(b) Result after the first FWI stage using 3 s long data.

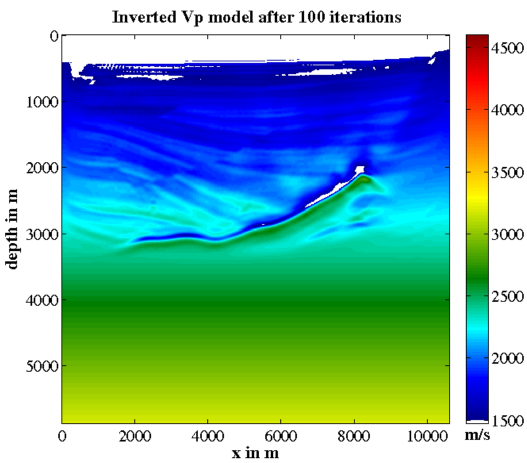

(c) Result after the second FWI stage using 4 s long data.

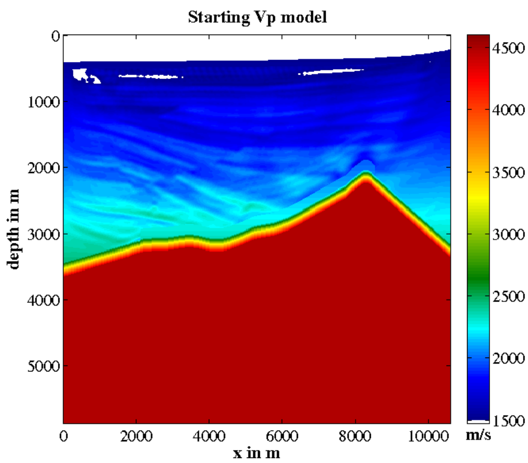

(d) Starting model for the third FWI stage: corrected artefacts above salt and smoothed transition zone included.

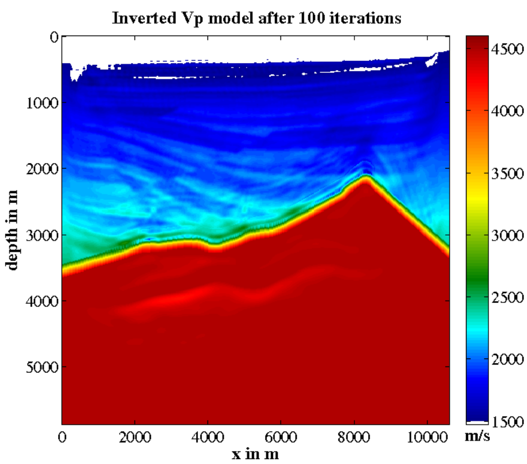

(e) Result after the third FWI stage using 4.8 s long data.

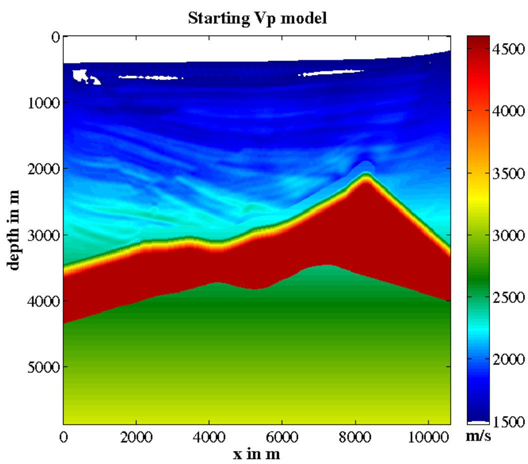

(f) Starting model for the fourth FWI stage: subsalt area is flooded with gradient.

Figure 5: P-wave velocity model at different stages of the modified Flooding Technique.

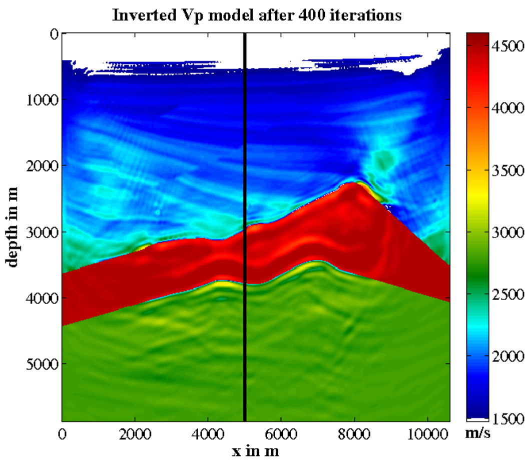

(a) Inversion result after 400 iterations, original Flooding Technique.

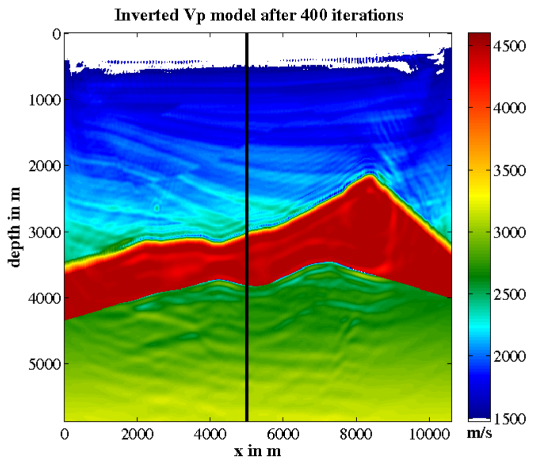

(b) Inversion result after 400 iterations, modified Flooding Technique.

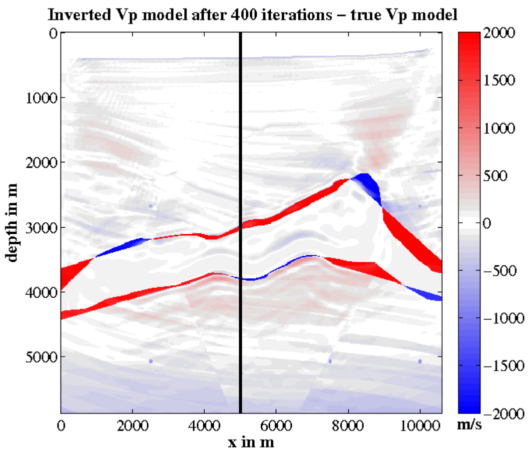

(c) Difference plot: result after FWI minus true model, original Flooding Technique.

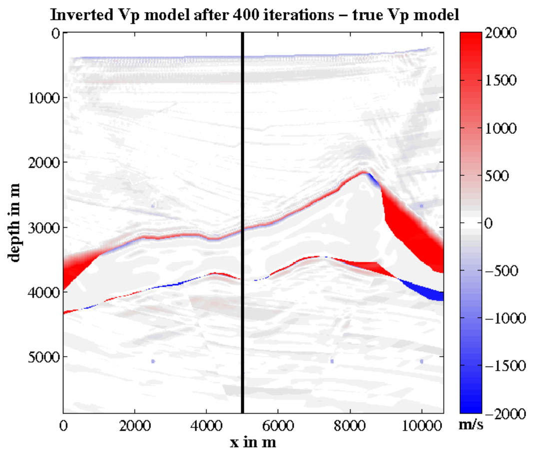

(d) Difference plot: result after FWI minus true model, modified Flooding Technique.

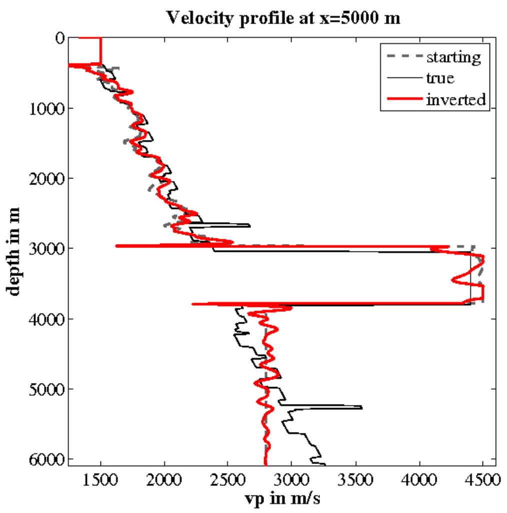

(e) Profile of v_P models located at the black vertical line in Figure 6(c), original Flooding Technique.

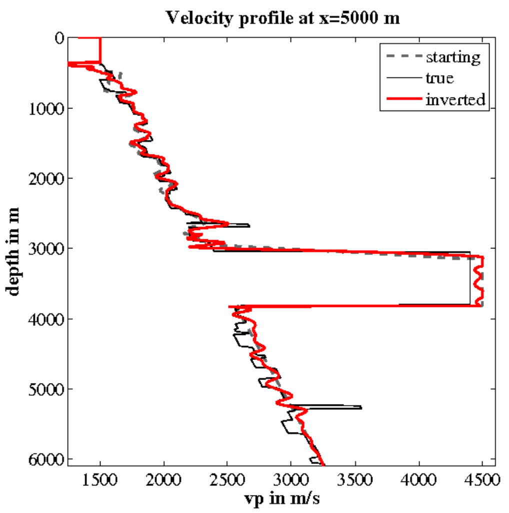

(f) Profile of v_P models located at the black vertical line in Figure 6(b), modified Flooding Technique.

Figure 6: Analysis of the FWI results obtained with the original and modified Flooding Technique.

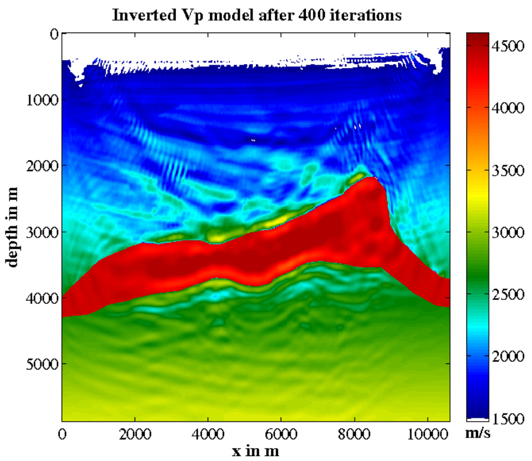

(a) V_P FWI result after 400 iterations using modified parameter.

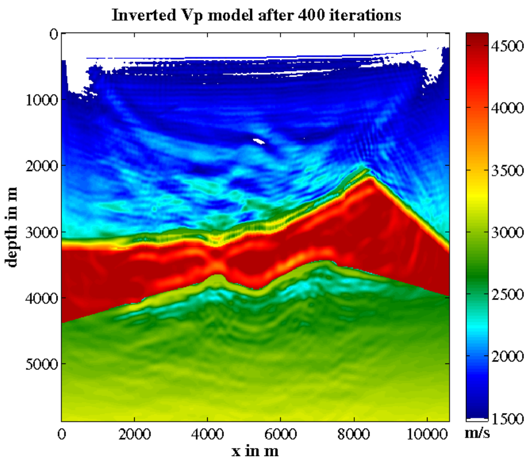

(b) FWI result after 400 iteration using modified Flooding Technique.

Figure 7: Results of the acoustic inversion with elastic data.

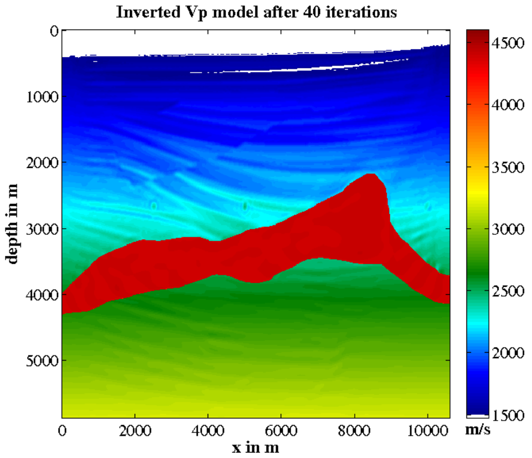

(a) V_P model after acoustic FWI with acoustic data (after 40 iterations).

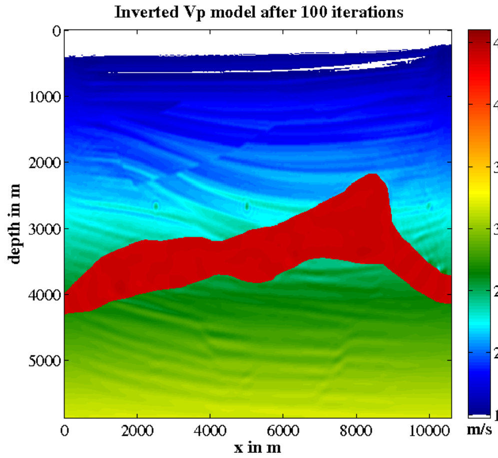

(b) V_P model after acoustic FWI with acoustic data (after 100 iterations).

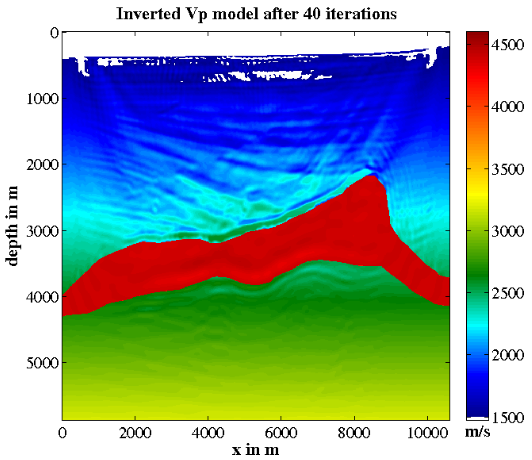

(c) V_P model after acoustic FWI with elastic data (after 40 iterations).

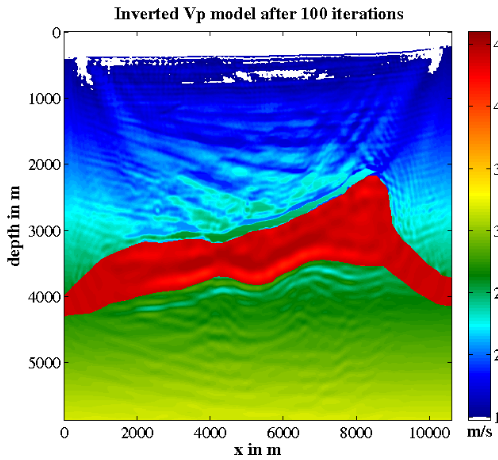

(d) V_P model after acoustic FWI with elastic data (after 100 iterations).

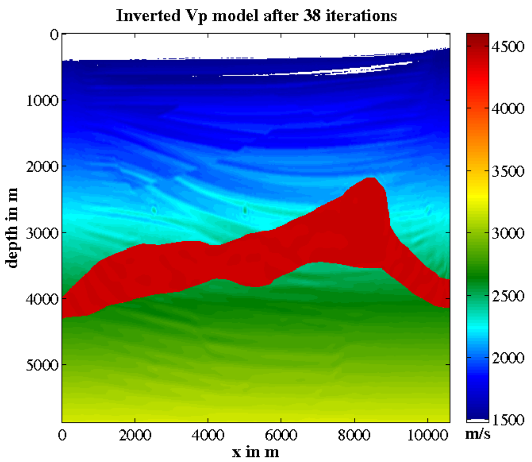

(e) V_P model after elastic FWI with elastic data (after 38 iterations).

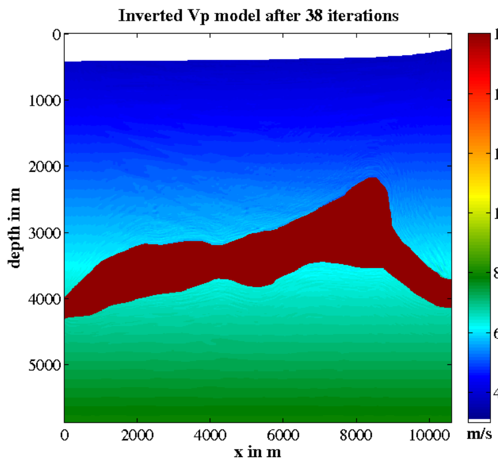

(f) V_S model after elastic FWI with elastic data (after 38 iterations).

Figure 8: Comparison of the results of the acoustic and elastic FWI with acoustic and elastic data (no frequency filtering; true density model).